2012

Synthesis of Mixed Metal Trinuclear Cluster of Molybdenum and Tungsten and Their Electrochemistry in Ionic Liquids

Jessica Ann Davis
Wright State University

SYNTHESIS OF MIXED METAL TRINUCLEAR CLUSTER OF MOLYBDENUM AND TUNGSTEN AND THEIR ELECTROCHEMISTRY IN IONIC LIQUIDS.

A thesis submitted in partial fulfillment
of the requirements for the degree of
Master of Science

By

JESSICA ANN DAVIS
B.A., Chemistry, East Carolina University, 2009

2012
Wright State University

WRIGHT STATE UNIVERSITY

GRADUATE SCHOOL

August 18, 2012

I HEREBY RECOMMEND THAT THE THESIS PREPARED UNDER MY SUPERVISION BY Jessica Ann Davis ENTITLED Synthesis of Mixed Metal Trinuclear Cluster of Molybdenum and Tungsten and Their Electrochemistry in Ionic Liquids BE ACCEPTED IN PARTIAL FULFILLMENT OF THE REQUIREMENTS FOR THE DEGREE OF Master of Science.

_____
Vladimir Katovic, Ph.D.
Thesis Director

_____
David Grossie, Ph.D., Chair
Department of Chemistry

Committee on
Final Examination

_____
Vladimir Katovic, Ph.D.

_____
David Grossie, Ph.D.

_____
David Dolson, Ph.D.

_____
Andrew Hsu, Ph.D.
Dean, School of Graduate Studies

ABSTRACT

Davis, Jessica A. M.S., Department of Chemistry, Wright State University, 2012. Synthesis of Mixed Metal Trinuclear Cluster of Molybdenum and Tungsten and Their Electrochemistry in Ionic Liquids

Research is being done to find a material to improve the efficiency of the ethanol fuel cell by using a platinum free catalyst. $Mo_2WO_2(O_2CCH_3)_6$ cluster was synthesized using $Mo_2(O_2CCH_3)_4$ dimer and Na_2WO_4. One ionic liquid, $EMImBF_4$, was synthesized using methylimidazolim and chloroethane in the first step, and EMImCl and $NaBF_4$ in the second step. The electrochemical properties of the ionic liquid and the metal cluster were studied. A potential window for the $EMImBF_4$ was found to be 3.2 V. The ionic liquid has a wider potential window, and allowed for the observation of the redox properties of $Mo_2WO_2(O_2CCH_3)_6$. The electrochemistry showed that $Mo_2WO_2(O_2CCH_3)_6$ cluster can be reduced to metal by reduction at -2.0 V. Finally, $Mo_2WO_2(O_2CCH_3)_6$ cluster was deposited onto a platinum electrode.

TABLE OF CONTENTS

TABLE OF CONTENTS (CONTINUED)

TABLE OF CONTENTS (CONTINUED)

LIST OF FIGURES

FIGURE PAGE

LIST OF FIGURES (CONTINUED)

LIST OF TABLES

TABLE PAGE

ACKNOWLEDGEMENT

I would like to thank Dr. Vladimir Katovic for the opportunity to join his research group. Thank you for all of your help, support, and guidance throughout this project. You have been a wonderful advisor.

I would like to think Kelsi Eberst and Amanda Lock for helping me in the lab.

I would like to thank Dr. David Dolson and Dr. David Grossie for
helping me through my thesis defense.

DEDICATION

To my grandfather, James Abbitt, who teaches me every day the true definition of strength and courage. I read a quote on time and I think it fits you so perfectly: “Be strong. Live honorably and with dignity. When you don't think you can, hold on”. I try to live my life everyday by your example. Your love and guidance has allowed me to become the woman I am today. Thank you for your constant and unfailing love, guidance, and support. I love you more than you will ever know.

To my family, thank you for your understanding and support. I could not have gotten through this experience without each and every one of you. I love you all.

I. INTRODUCTION

ALCOHOL FUEL CELL

Over the past decade, fuel cells have become a major area of research. Fuel cells are devices that convert chemical energy to electrical energy without the production of a significant amount of heat. The conventional fuels that are used right now are fossil fuels. They are formed through a natural process such as anaerobic decomposition of dead organisms. Fossil fuels take millions of years to form, so they are considered a non-renewable resource. The major use for the fossil fuels right now is as petroleum. The purpose of these fuels is to store energy that can be used at a later time to generate heat or do some form of work. There are many types of alternative fuels that are being used in fuel cells such as: methanol, ethanol, and hydrogen. An alternative fuel source could help the United States save some of their natural resources. The United States is currently depleting our reserves much faster than the new ones are being made. Figure 1 shows the consumption versus production rate of energy sources in the United States, according to the Energy Information Administration[21].

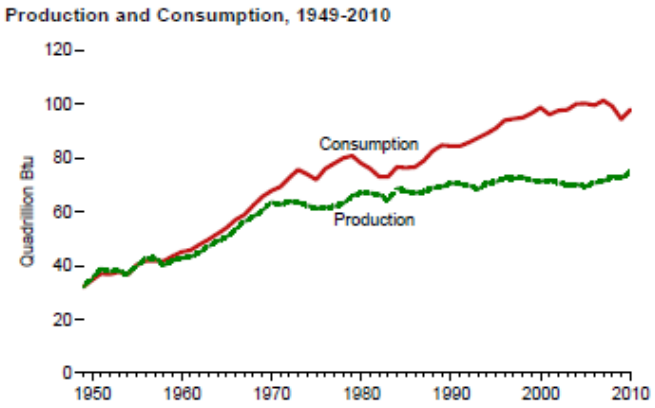

Figure 1. Consumption versus production of energy sources in United States

With gas prices rising and our natural resource supplies running out, it has become very evident that we need a new power source for portable and mobile applications. This is where an alternative fuel source, such as a fuel cell, would come into play. Figure 2 shows the major energy consumption source in the United States as of 2010, according to the Energy Information Administration[21]. It is clearly seen that petroleum is at the top of the list, while the renewable energy sources are at the bottom.

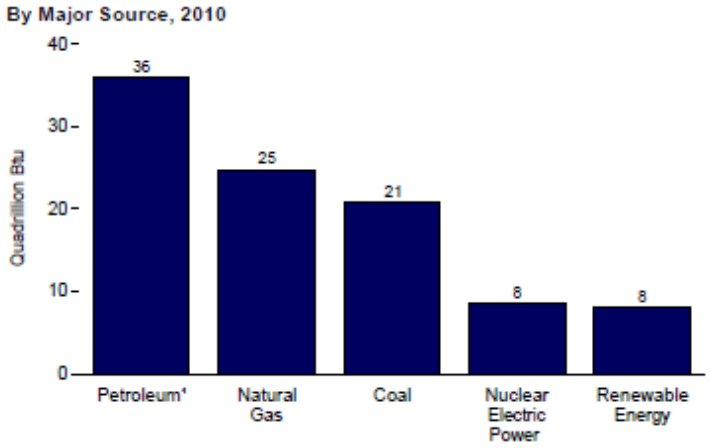

Figure 2. Major energy consumption source in the U.S. as of 2010

In 1838, Christian Friedrich Schönbein was the first to observe the fuel cell effect, the inverse electrolysis process. William Grove took Schönbein's findings and designed a gaseous voltaic battery in 1839. Direct alcohol fuel cells are now being explored extensively. The main types of direct alcohol fuel cells are: direct methanol fuel cell (DMFC) and direct ethanol fuel cell (DEFC). Both of these fuel cells are being used with a proton exchange membrane, (PEM).

METHANOL FUEL CELL

The direct methanol fuel cell has a few appealing qualities: it has the ability to use a high energy density; methanol is inexpensive and is commonly available. One of the major downfalls to the methanol fuel cell is its low power density and the large amount of metal catalyst that has to be used. The direct methanol fuel cell, also, has slower kinetics with the oxidation of methanol because the CO produced blocks the catalyst sites. The last issue with this fuel cell is methanol is crossing over the membrane and creating mixed potentials at the cathode. This in turn causes low efficiency of this methanol fuel cell. Figure 3 shows the methanol fuel cell.

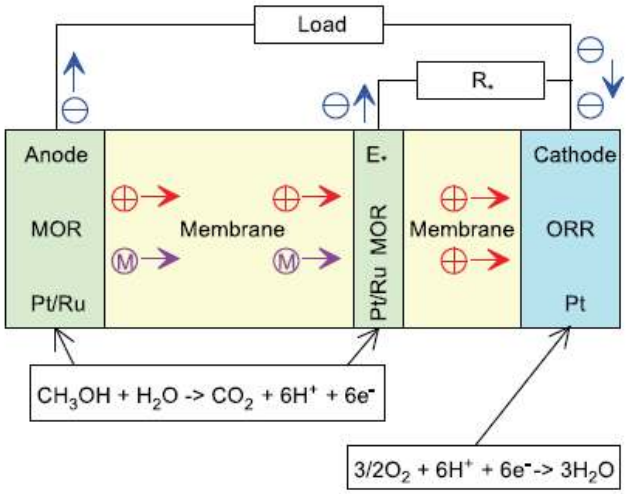

Figure 3. Methanol fuel cell

ETHANOL FUEL CELL

Tremendous efforts have been made to produce an efficient direct ethanol fuel cell. Its biggest competitor is the direct methanol fuel cell. The direct ethanol fuel cell does have some clear advantages, however. Ethanol is produced from renewable resources such as corn and wheat. Ethanol has a higher theoretical mass energy density. It is less toxic than methanol, and it is cheaper in production. These are two of the main reasons research done on the direct ethanol fuel cell has skyrocketed in the last few years. Figure 4 shows the ethanol fuel cell.

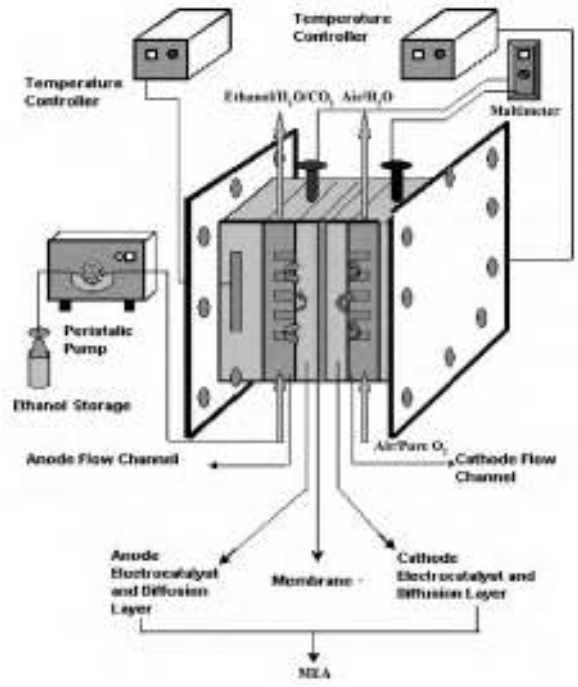

Figure 4. Ethanol Fuel Cell.

In a direct ethanol fuel cell, the ethanol is oxidized by a catalyst to form carbon dioxide. Water is produced at the cathode due to protons being transported across the proton

exchange membrane. The protons at the cathode, then, react with oxygen to produce water. Power is provided to connected devices due to the transportation of protons from the anode to the cathode. Table 1 shows the reactions that take place in the ethanol fuel cell.

Anode (Oxidation)	$C_2H_5OH + 3\ H_2O \rightarrow 12\ H^+ + 12\ e^- + CO_2$
Cathode (Reduction)	$3\ O_2 + 12\ H^+ + 12\ e^- \rightarrow 6\ H_2O$
Overall reaction	$C_2H_5OH + 3\ O_2 \rightarrow 3\ H_2O + 2\ CO_2$

Table 1. Reactions in the ethanol fuel

The goal is to completely oxidize the ethanol to carbon dioxide. If this does not occur, then efficiency is going to be reduced. At low temperatures, a Carbon-Carbon bond has to be broken to completely oxidize ethanol. This is one of the limiting factors in the development of an efficient direct ethanol fuel cell. The oxidation of ethanol involves 12 electrons, whereas the oxidization of methanol only involves 6 electrons.

Alcohols have energy density close to that of hydrocarbons and gasoline. This is what makes alcohols an alternative energy carrier that could be used in automobiles. Table 2 shows the thermodynamics of certain alcohols.

Thermodynamic data associated with the electrochemical oxidation of some alcohols (under standard conditions)

Fuel	ΔG_f° (kJ/mol)	E_f° (V vs. SHE)	ΔG° (kJ/mol)	E_{cell}° (V)	W_e(kWh/kg)	ΔH° (kJ/mol)	η_{rev}
CH_3OH	−9.3	0.016	−702	1.213	6.09	−726	0.967
C_2H_5OH	−97.3	0.084	−1325	1.145	8.00	−1367	0.969
C_3H_7OH	−281	0.162	−1853	1.067	8.58	−2021	0.916
C_4H_9OH	−464	0.200	−2381	1.029	8.93	−2676	0.890

Table 2. Thermodynamic data for certain alcohols.

Currently it is cheaper to produce gasoline, than to produce the equivalent amount of ethanol. Ethanol is being produced by the fermentation of glucose by yeast. Research efforts are being made to improve the ethanol production process. Cell free ethanol production could solve this problem. Eduard Buchner found that sugar could be converted to ethanol from cell free extracts of yeast in 1897. Research is still being done to improve this process. This, however, is not the only issue with the direct ethanol fuel cell.

Platinum is, currently, being used as a catalyst in the direct ethanol fuel. It is showing poor efficiency due to its difficulty to oxidize ethanol in an acid medium. Research is being done to see if the efficiency can be increased by using an alkaline medium. Platinum is poisoned during the oxidation process by CO, which is made from the dissociation of organic molecules. This is what causes the reactivity of platinum to reduce. Platinum is an expensive metal, as well. It costs $13,000 per 100 grams, currently. Due to the efficiency and the cost, the option of using a platinum free catalyst is now being explored.

METAL CLUSTER COMPOUNDS

Metal clusters have been found to be good catalysts, and research is being done to use them to replace platinum as the catalyst in the ethanol fuel cell. Each metal atom in the cluster is bonded to the neighboring metal atom by a metal-metal bond. Metal atoms in a metal cluster are in close proximity to one another. This allows them to bind small molecules, which facilitates the multi-electron reduction process.

F. A. Cotton coined the term “metal-atom-cluster”, which describes compounds with metal-metal bonds. One of the first examples of a metal cluster was $[Mo_6Cl_8]^{4+}$, which is

shown in Figure 5. It consists of 6 metal atoms forming an octahedral cluster where each triangular Mo_3 is capped with a chloride ion. The transitional metal clusters have half filled s and d orbitals, which causes maximum binding energies to occur at the center of the transition series. The ligands that surround the metal attempt to modify the electronic configuration while achieving their maximum binding energy.

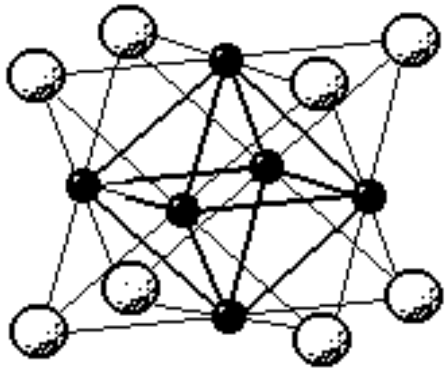

Figure 5. Structure of $[Mo_6Cl_8]^{4+}$.

Polynuclear metal complexes are inorganic complexes that do not have a direct metal-metal bond. Metal atoms in these compounds are held together by bridging ligands, which is shown in Figure 6. Some common inorganic bridging ligands are: OH^-, SH^-, NH_2^-, and CO.

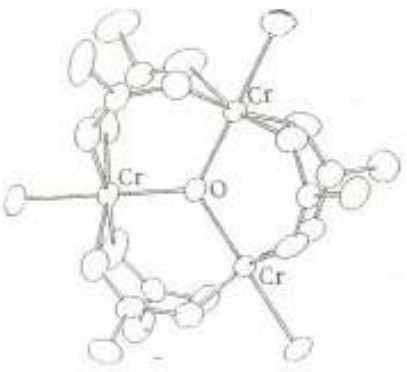

Figure 6. Polynuclear complex, $Cr_3O(CH_3CO_2)_6(H_2O)_3^+$

There are two types of transition metals that form these metal clusters: late transition metals and early transition metals. Early transition metals exhibit high stability, they are inert, and have very strong M-ligand bonds. They contain metal atoms in higher oxidation states and Π-donor ligands. The higher oxidation states will stabilize the metal cluster more efficiently. Early transition metals have bond strengths twice as strong as the late transition metals, as seen in Table 3.

metal	$D°(M^+–O)$	$D°(M–O)$	metal	$D°(M^+–O)$	$D°(M–O)$
Sc	159 ± 7	161.5 ± 3	Mn	57 ± 3	85 ± 4
Ti	161 ± 5	158.4 ± 2	Fe	69 ± 3	93 ± 3
V	131 ± 5	146 ± 4	Co	64 ± 3	87 ± 4
Cr	85.3 ± 1.3	110 ± 2	Ni	45 ± 3	89 ± 5

Table 3. Bond Strengths for Transition Metals (kcal/mol).

EARLY TRANSISTION METALS

Early transition metals can form double, triple, and quadruple metal-metal bonds as well as the typical single bond. Figure 7 shows an example of an early transition metal cluster.

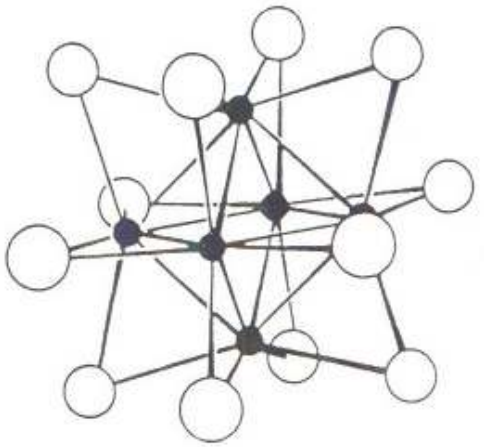

Figure 7. Early transition metal, $Ta_6Cl_{12}^{2+}$

LATE TRANSITION METALS

Late transition metals contain metals in low oxidization states, mostly zero, -1, or +1. They contain Π-acceptor ligands that withdraw electrons by Π-back-bonding. Late transition metals are highly reactive oxidizing agents that have weaker M-ligand bonds. They are formed by metals like: rhodium, ruthenium, and iridium and contain nitrosyl, cyano, phosphine, or carbonyl ligands. Carbonyl is the most common ligand. It occupies the terminal, edge-bridging, or face-capping locations in the cluster, and stabilizes the low oxidization state of the cluster. Figure 8 shows an example of a late transition metal.

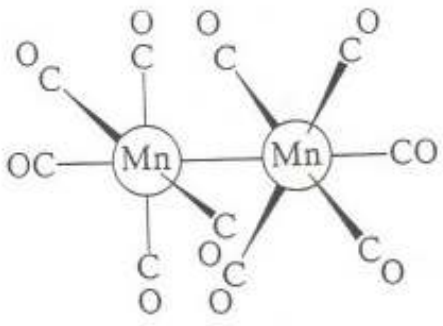

Figure 8. Late transition metal, $[Mn_2(CO)_{10}]$

TRINUCLEAR METAL CLUSTERS

Trinuclear clusters are the most common type of metal cluster. They are formed by both early and late transition metals as well as metal carbonyls. Early transition metals have bond orders of 2/3 to 1 due to their low oxidation state. Some examples of these early transition metals are: tungsten, titanium, and molybdenum. Rhenium trihalides are the most common trinuclear metal cluster. The first known rhenium cluster with an iodide

bridge was discovered in 1991 by Jung and Meyer[21]. Each rhenium atom is bonded to another rhenium atom by metal-metal bonds with the iodide bridge between them. These clusters have three different geometries: triangular, octahedral, and $[M_6X_{12}L_6]$ type. Figure 9 shows each of the three types of geometries: A. Triangular, $[Re_3Cl_{12}]^{3-}$, B. Octahedral, $[Mo_6Cl_8L_6]^{4+}$, C. $[M_6X_{12}L_6]$, $[Nb_6Cl_{12}L_6]^{2+}$. For the most part, they will either have tetrahedral or octahedral geometry.

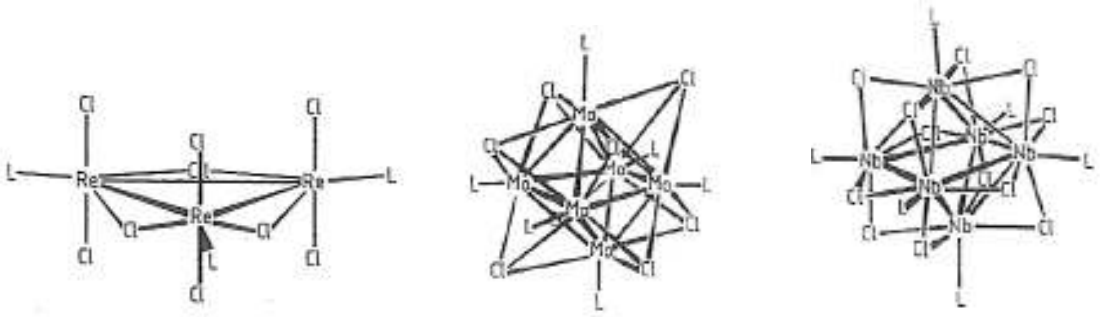

A. Triangular, $[Re_3Cl_{12}]^{3-}$ B. Octahedral, $[Mo_6Cl_8L_6]^{4+}$ C. $[M_6X_{12}L_6]$,$[Nb_6Cl_{12}L_6]^{2+}$.

Figure 9. Geometries for trinuclear clusters.

BINUCLEAR METAL CLUSTERS

Binuclear metal clusters have a multiple metal-metal bonds, and bond orders up to 4. These clusters are seen most commonly in $Re_2X_8^{2-}$ ions and in binuclear carboxylates. Figure 10 shows an example of a binuclear cluster. This was the first example of a quadruple bond. A quadruple bond is caused by one σ bond, two π bonds, and one δ. An overlap of d_{yz} and d_{xz} on each of the Re atoms occurs as a result of the σ bond. The $[Re_2Cl_8]^{2-}$ ion has a short bond distance between the rhenium atoms. The chloride ions are in an eclipsed position, which allows positive overlap of the d_{xy} orbitals, which forms the forth bond.

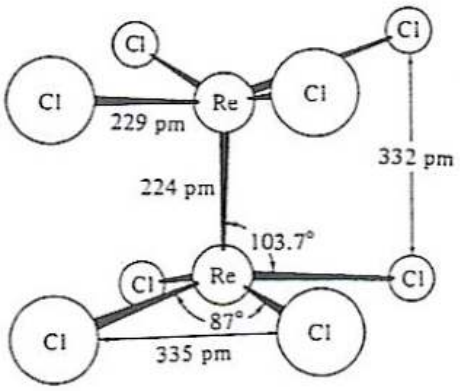

Figure 10. Binuclear metal complex, $[Re_2Cl_8]^{2-}$

The formation of the quadruple bonds on the two Re atoms is shown in the MO diagram in figure 11.

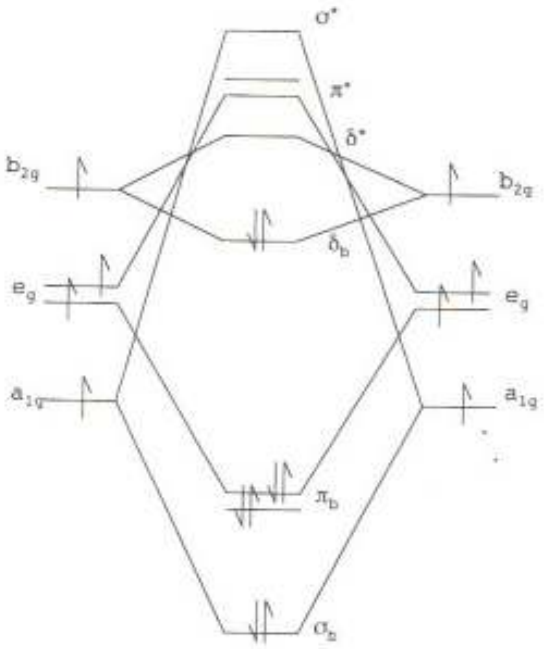

Figure 11. MO diagram for $[Re_2Cl_8]^{2-}$

TETRANUCLEAR METAL CLUSTERS

The first tetranuclear metal cluster, $[Co_4(CO)_{12}]$, was discovered in 1910[16]. Most tetranuclear metal clusters are found among carbonyl clusters. A few are, even, found among halides and oxides. Tetranuclear metal clusters have six different types of geometries that they can be found in: tetrahedron, butterfly, square planar or rectangle, planar butterfly, spiked triangle, and straight or bent chain. Each type of geometry is defined by the number of metal-metal bonds the cluster contains. Figure 12 shows an example of each of the geometries of the tetranuclear clusters: A. Tetrahedron, B. Butterfly, C. Planar butterfly, D. Spiked triangle, E. Square planar or rectangle, and F. Straight or bent chain.

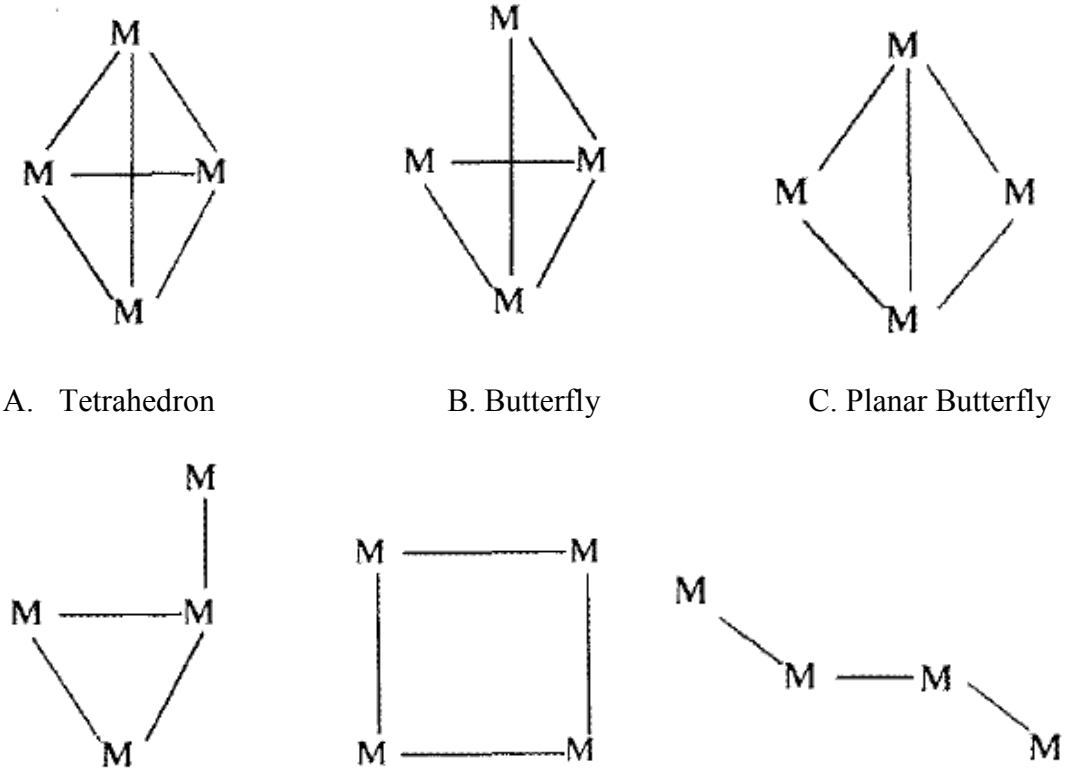

A. Tetrahedron B. Butterfly C. Planar Butterfly

D. Spiked Triangle E. Square planar or rectangle F. Straight or bent chain

Figure 12. Geometries of the tetranuclear clusters

HEXNUCLEAR METAL CLUSTERS

Hexanuclear metal clusters contain six metal atoms. There are two types of hexanuclear metal clusters: an octahedral cluster formed from six Mo atoms and an octahedron cluster with twelve halide ligands on the edge of each cluster. In the octahedral cluster, three of the six metal atoms are bridged by eight chloride ligands. The clusters are formed by single bonding to several other metal atoms or by multi-bonding to another metal atom, because the metal has such a low oxidation state. One of the first examples of a metal cluster was $[Mo_6Cl_8]^{4+}$, which is a hexanuclear metal cluster. It is an octahedral cluster where each triangular Mo_3 is capped with a chloride ion. Figure 13 shows the $[Mo_6Cl_8]^{4+}$ hexanuclear metal cluster. Some of the first hexanuclear metal clusters to be synthesized contained molybdenum, tantalum, and niobium.

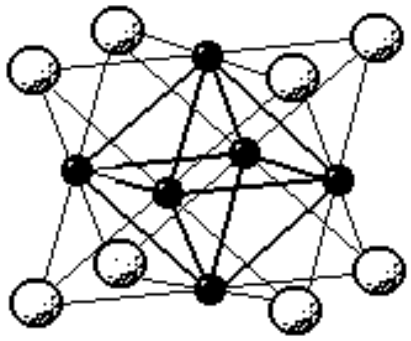

Figure 13. Hexanuclear cluster, $[Mo_6Cl_8]^{4+}$

MOLTEN SALTS

A molten salt is an inorganic salt, composed of cations and anions, which melts or becomes a liquid above its melting point. These salts are being used in electrochemistry due to the fact that they are stable at high temperatures, they are ionic and conductive, and they transfer heat. One of the most common examples of a molten salt is NaCl, which

becomes molten or a liquid above 800^{o}C. One of the most common uses for these salts is as solvents for the electrolytic production of metals. They have extremely high melting temperatures (NaCl, for example, has a melting temperature around 800^{o}C). Extreme care and safety measures have to be taken when dealing with these salts due to those high temperatures. They are, also, corrosive, hydroscopic, and sometimes hard to characterize.

IONIC LIQUIDS

Ionic liquids are molten salts that are in liquid form at or near room temperature (melting point below 100^{o}C). These liquids are, also, known as: low temperature molten salts, ambient temperature molten salts, and liquid organic salts. They are most commonly called ionic liquids, however. They are extremely thermally stable, have low vapor pressures, good electrolytic properties, and they are tunable. The physical and chemical properties of these liquids can be tuned by changing the cation or anion that is selected to be used. There are, currently, 10^{18} different combinations of cations and anions that can be used to tune these ionic liquids. Ionic liquids can contain organic or inorganic ions or a combination of both. Typically, a large organic cation with a smaller inorganic anion is used. The first room temperature ionic liquid, ethylammonium nitrate, was discovered in 1914 by Paul Walden.

Figure 14 shows the synthesis of an ionic liquid, $EMImBF_4$. Almost 20 years ago, the United States Air Force synthesized this ionic liquid. It, also, shows the tunablility of these ionic liquids. In the synthesis, the ionic liquid is tuned by changing the anion from Cl^- to BF_4^-.

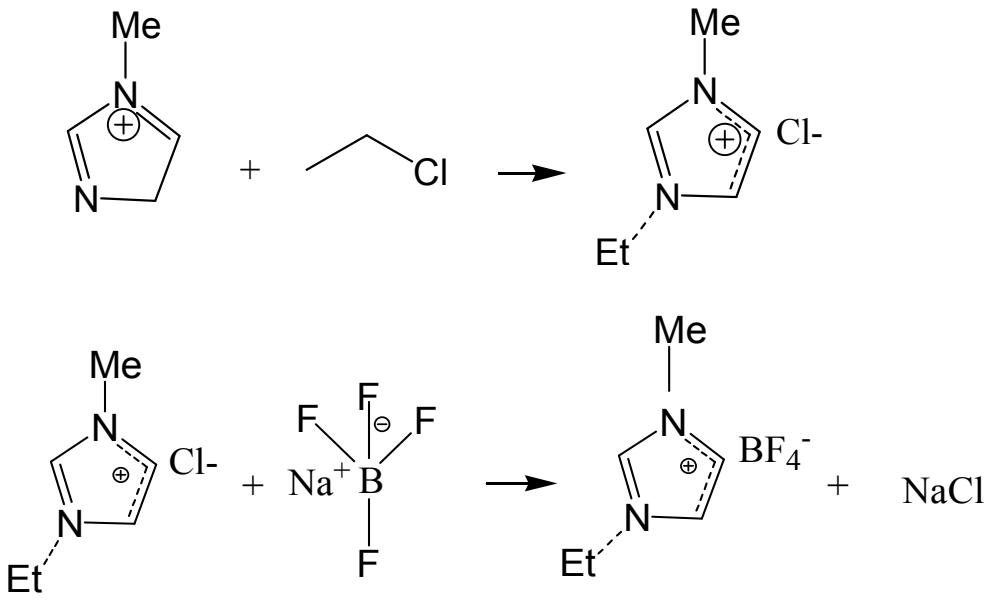

Figure 14. Synthesis of ionic liquid, $EMIBF_4$

Here are some common possibilities of cations and anions that can be selected to make these ionic liquids:

Cations:	
Methyl	MMImCl
Ethyl	EMImCl
Propyl	PMImCl
Isopropyl	iPMImCl
Anions:	
Hexafuorophosphates	PF_6^-
Tetrafluoroborate	BF_4^-
Aluminate Halide	AlX_4^-

Table 4. Cations and anions that can be selected to make ionic liquids

The role of the cation and anion are extremely important when deciding what properties the ionic liquid is going to demonstrate. The cation is extremely important because the attraction between the cation and the anion is the driving force of the reactions. These ions influence how the ionic liquid is going to act and react. Figure 15 shows some of the common cations that are used today when making these liquids, and Table 5 shows some of the common anions that are used. Usually a large organic cation is selected with a smaller inorganic anion.

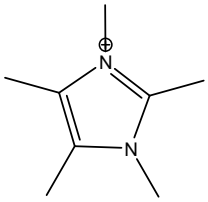

Imidazolium

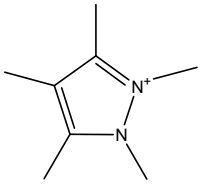

Pyrazolium

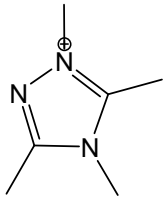

Triazolium

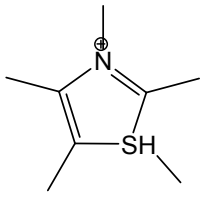

Thiazolium

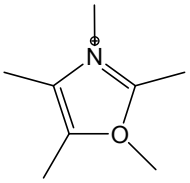

Oxazolium

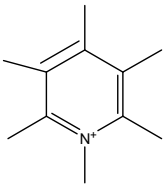

Pyridinium

Figure 15. Common cations used in ionic liquid.

Inorganic	**Organic**
BR_4^-	Sulfonate $^-O\text{-}(SO_2R)$
PR_6^-	Imide $^-N\text{-}(SO_2R)_2$
	Methide $^-C\text{-}(SO_2R)_3$

R is a halide

Table 5. Common anions used in ionic liquids

Ionic liquids have strong ion-ion interactions. These interactions contribute to the thermal stability of these liquids. Ionic liquids are thermally stable up to 450^0C. Figure 16 shows a thermogravimetric analysis for four ionic liquids, $EMImBF_4$, $EMPBF_4$, $EMPCF_3SO_3$, and $DMFPBF_4$, and demonstrates their thermal stability[20]. It can be seen from Figure 16 that the liquids start to decompose and lose mass around 360^oC to 450^oC.

These ionic liquids have been found to be beneficial solvents in a wide range of applications due to their properties. They are non-toxic, non-volatile, non-corrosive, and are highly conductive. These properties are the reason these ionic liquids are being referred to as the new "green solvents".

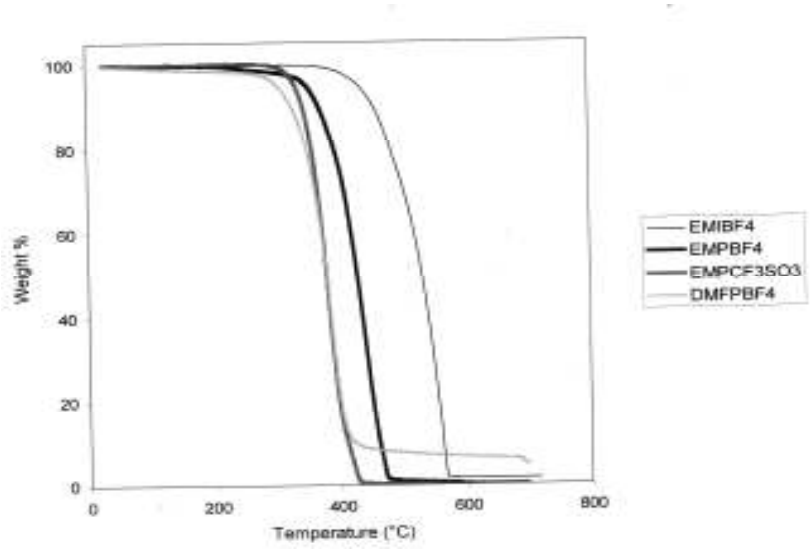

Figure 16. Thermogravimetric analysis for ionic liquids

USES OF IONIC LIQUIDS

In the last decade, ionic liquids have been utilized in a wide range of research fields. They are being used in the electrochemistry field as batteries and photoelectrochemical cells. They are, also, being used in the organic chemistry field in reactions such as the Diels-Alder reaction. Ionic liquids are being utilized as high/low temperature lubricants

and hydraulic fluids. The pharmaceutical industry is now looking into these liquids for numerous uses such as a possible treatment of cancer.

ELECTROCHEMICAL METHODS

Electrochemical methods are analytical techniques that study the electrical properties of an analyte in an electrochemical cell. There are three main types of electrochemical methods: Potentiometry, Coulometry, and Voltammetry. Potentiometry measures the potential of the cell as a function of the analyte. Coulometry measures the electrical charge during electrolysis. Voltammetry, which will be the technique of choice, is the measure of applied potential and current.

POTENTIMETRY

Potentiometry is an electrochemical method that measures the potential of an electrochemical cell with little or no current passing through the sample. Two types of electrodes are used during this method: indicator electrode and reference electrode. The indicator electrode responds to change in activity in the analyte. A pH electrode is probably the most common type of indicator electrode. A potential between the indicator electrode and the analyte is measured relative to the reference electrode. The most commonly seen reference electrode is the ion-selective electrode, or ISE.

COULOMETRY

Coulometry determines the amount of electricity used during electrolysis by measuring the electrical charge. There are two types of coulometry: potentiostatic coulometry and coulometric titration. Potentiostatic coulometry uses a working electrode that is kept at a constant potential and the current that flows through is measured. The potential that is applied fully reduces or oxidizes the substrate in a solution. When the substrate is

consumed the current decreases and approaches zero. Coulometric titration uses a constant current to identify the concentration of an unknown species. Current is applied to an unknown solution until all species are oxidized or reduced.

VOLTAMMETRY

Voltammetry obtains information about an analyte by measuring applied potential and current. There are several types of voltammetry: linear sweep voltammetry, cyclic voltammetry, and anodic and cathodic stripping voltammetry. Linear sweep voltammetry measures the current at the working electrode as a function of applied potential between the working and reference electrode. In cyclic voltammetry, the potential of the working electrode is changed up to a certain point and then reversed in the opposite direction linearly versus time. It is similar to linear sweep voltammetry, except when it reaches a set potential the working electrode's potential is inverted. Anodic and cathodic stripping voltammetry is a method for trace analysis of metal cation and anions.

CYCLIC VOLTAMMETRY

Cyclic voltammetry will be used to measure the potential of a working electrode that will consist of a molybdenum and tungsten metal cluster versus time. The redox state of this metal cluster will be observed. This is one of the most widely used methods in electrochemistry. There are three electrodes that are utilized in this method: the reference electrode, working electrode, and the auxillary electrode. Figure 17 shows the three electrodes used in the cell.

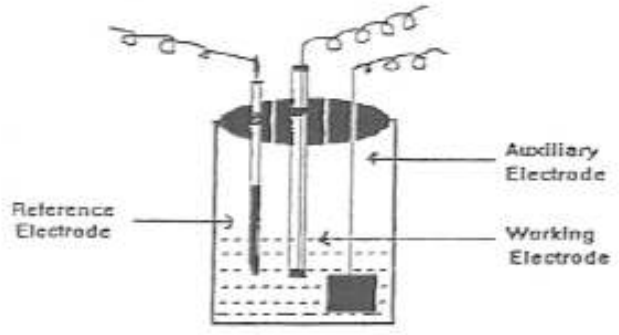

Figure 17. The three electrodes used in the cell.

Cyclic voltammetry is an extremely useful and popular technique in the electrochemistry field. It is one of the first techniques that an electrochemist will decide to use due to the usefulness of the data it provides. It is a very simple and versatile technique. Cyclic voltammetry is used to identify the oxidation and reduction properties of compounds. The cyclic voltammetry method is similar to the linear sweep method mentioned before. The only difference between the two methods is the point where they stop collecting data. The linear sweep method stops collecting data once the potential is reached. The cyclic voltammetry method, however, reaches the potential and then reverses back to the original potential. The cyclic voltammetry method starts by changing the potential of the working electrode linearly compared to that of the reference electrode and the resulting current is measured. The potential changes linearly and then reverses back to the original potential. The forward part of the scan is the reduction sweep. This is where the initial potential is more positive than the final potential. The reverse cycle is the oxidation sweep. Figure 18 shows an example of a cyclic voltammetry scan.

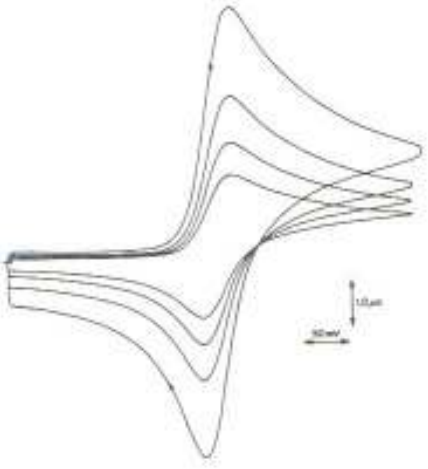

Figure 18. Cyclic voltammetry scan

As seen in Figure 18, the forward sweep shows the current that is caused by the reduction, and then the reverse sweep shows the current that is caused by the re-oxidization of the compound that was formed in the forward sweep. This information gives insight on how the compound is reduced and re-oxidized. This is the most powerful quality of the cyclic voltammetry method. It quickly gives information on the reaction potential of redox process for a certain compound and the kinetics of the electron-transfer of the reactions. It, also, gives insight into the steps in the chemical reactions including the electron transfer step. You get an overall picture of the electrochemical process and its properties.

A cyclic voltammogram, like the one in Figure 18, has four measurable quantities: cathodic peak current or I_{pc}, anodic peak current or I_{pa}, cathodic peak potential or E_{pc}, and anodic peak potential E_{pa}. All of the quantities are, then, used to calculate the standard reduction potential of an electrochemical reaction, the rate constants of the steps in the reaction, and the number of electrons transferred during the reaction.

There are three types of systems that are seen in cyclic voltammetry: a reversible system, a quasi reversible system, and an irreversible system. Figure 19 shows the difference between the reversible system and the quasi reversible system. A quasi reversible system is caused by the magnitude of the electron exchange rate being similar to that of the cyclic voltammetry. In an irreversible system the current on the reverse sweep will not show up.

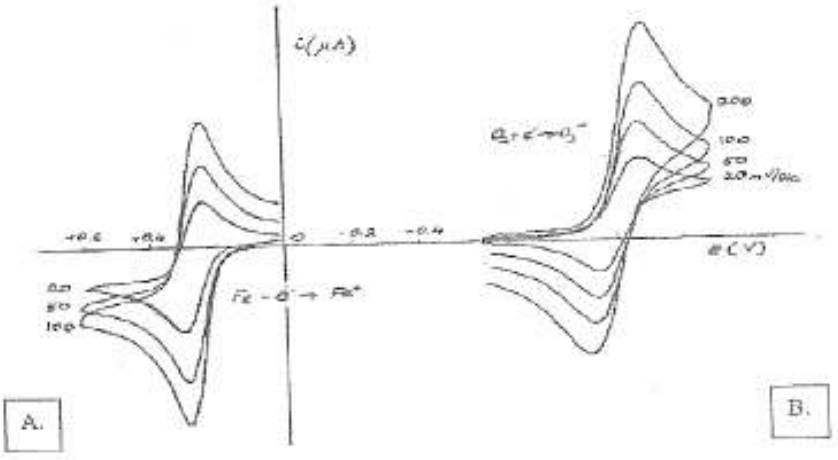

A. Reversible system B. Quasi reversible system

Figure 19. Reversible and Quasi reversible system

I. EXPERIMENTAL

MATERIALS

1-Methylimidazole (99+%) was purchased from Sigma Aldrich. It was purified by a distillation under vacuum (13.8 mmHg). Chloroethane gas (99.7+%) was obtained from Aldrich Chemical Company and was used as recieved. Sodium Tetrafluoroborate (95%) was received from Alfa Aesar and was used as received. Acetonitrile, gradient grade +99.0%, was purchased from Fisher Scientific and used as received. Diethyl Ether was obtained from Fisher Company. Sodium tungstate, acetic anahydride, triethylamine, molybdenum hexacarbonyl, and Dowex 50X2-200 ion exchange resin were purchased from Sigma Aldrich. Acetic Acid was purchased from Aristar. Trifluoromethanesulfonic acid (99.5%) was obtained from Alfa Aesar.

SYNTHESIS OF 1-ETHYL-3-METHYLIMIDAZOLIUM CHLORIDE

1-Methylimidazole (99%) was distilled at 90-100^{o}C under vacuum (13.8 mmHg). In an I^2R glove bag that was filled with nitrogen gas, 48.7 grams of chloroethane was condensed into a reaction flask, using a bath of liquid nitrogen/ethanol solution at a temperature of -30 to -50 ^{o}C. 56.8 g of 1-Methylimidazole was added to the reaction flask, and it was sealed with a Teflon screw cap, and removed from the glove bag. The reaction mixture was heated at 35^{o}C for 7 days. A box was put over the reaction flask to keep light out, because the light could cause the formation of impurities. After the

reaction was complete, two layers were visible, the reaction flask was cooled in the refrigerator overnight. Once the white crystals of 1-Ethyl-3-Methylimidazole Chloride were formed, the liquid on top was decanted and the crystals were dissolved in acetonitrile. EMImCl was precipitated by the addition of diethyl ether after cooling in the refrigerator. The white crystals of EMImCl were obtained. The product was filtered under nitrogen gas using a Schlenk filteration flask. The crystals were, then, dried under vacuum overnight. The dry EMImCl was stored under nitrogen until later use.

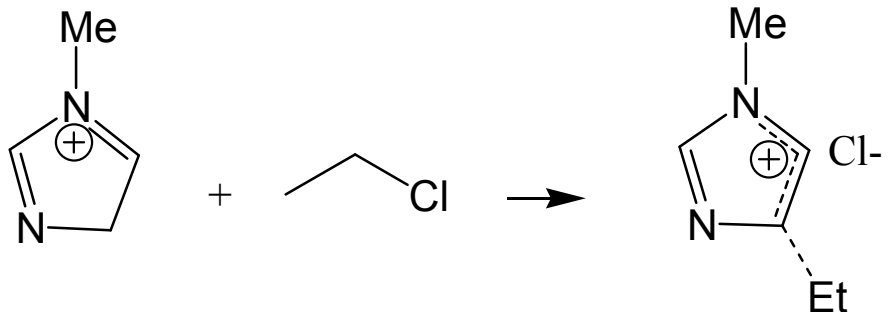

SYNTHESIS OF 1-ETHYL-3-METHYLIMIDAZOLIUM TETRAFLOUROBORATE

$EMImBF_4$ was obtained by an ion exchange reaction between 1-Ethyl-3-Methylimidazolium Chloride and Sodium Tetrafluoroborate in water. 0.6975 moles of -Ethyl-3-Methylimidazolium Chloride (101.92 g) was dissolved in 300 mL of distilled water. Then, an equimolar amount of Sodium Tetrafluoroborate (76.580 g) was dissolved in 300 mL of distilled water. The two solutions were combined, and the combined solution was allowed to stir on a stirring plate for 24 hours at room temperature. After complete reaction, the water was removed from the solution by rotatory evaporation under vacuum at 80 ^{o}C. Once the water was removed, the solution was filtered using a fine porosity frit filter funnel to remove any NaCl. The excess chloride in the solution

was removed by adding a known amount of $AgBF_4$. The end of the reaction was determined using potentiometric titration. An Ag | AgCl, $HgSO_4$ | Hg reference electrode was used to measure the equivalence point. An equivalence point of 200 mV of the Ag | AgCl electrode was reached. The equivalence point can be seen on the titration curve in Figure 20.

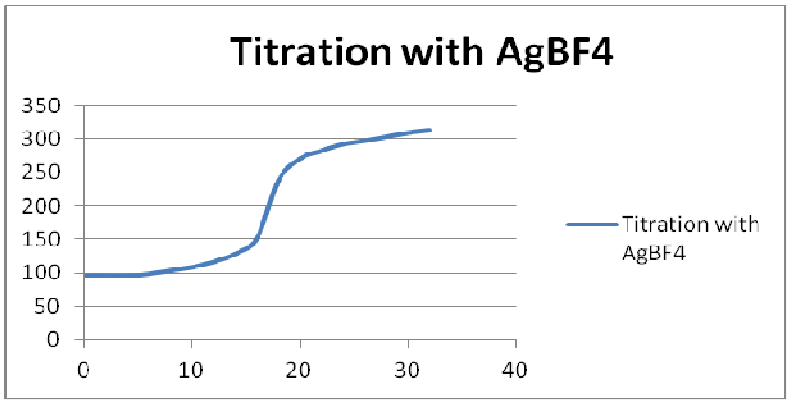

Figure 20. Titration curve of chloride ion in $EMImBF_4$ with silver nitrate.

The solution was, then, evaporated on the rotatory evaporation system at 80 ^oC under vacuum. After filtering the solution, to remove AgCl, 500 mL of acetonitrile was added, and the solution was evaporated under vacuum to obtain $EMImBF_4$ without traces of chloride ions. 1-Ethyl-3-Methylimidazolium Tetraflouroborate was tested for the presence of chloride ions with $AgBF_4$. The solution was, finally, dried on high vacuum to remove any excess water.

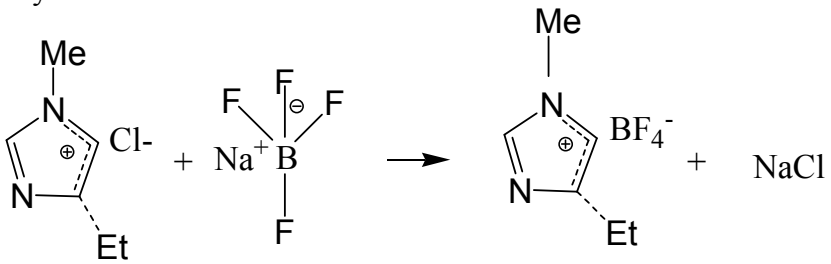

SYNTHESIS OF $Mo_2(O_2CCH_3)_4$

Quadruply bonded molybdenum dimer was synthesized from $MoCO_6$ in acetic acid. 4 mL of acetic anhydride and 9 mL of acetic acid were prepared. They were mixed with 16.069 g of molybdenum hexacarbonyl and put in a Schlenk flask equipped with a condenser and connected to a gas bubbler. The Schlenk flask was pumped with nitrogen after vacuum was applied to remove oxygen. Oxygen will oxidize the solid molybdenum hexacarbonyl. The reaction proceeds stoichiometrically according to:

$$2\ Mo(CO)_6 + 4\ CH_3COOH \rightarrow Mo_2(O_2CCH_3)_4 + 12\ CO + 2\ H_2$$

The mixture was refluxed while heating until all CO evolution ceased. Yellow crystals were obtained and after cooling to room temperature. The $Mo_2(O_2CCH_3)_4$ was filtered using Schlenk technique under nitrogen. The crystals were, then, transferred in a dry box to a pre-weighed vial. 8.41 g of product was obtained.

SYNTHESIS OF $[Mo_2WO_2(O_2CCH_3)_6(H_2O)_3](CF_3SO_3)_2$

The Mo_2W dimer was prepared by reacting Na_3WO_3 and $Mo_2(O_2CCH_3)_4$. 3.230 g of sodium tungstate dehydrate was prepared with a mortar and pestle and placed in a 200 mL schlenk flask that contained a deaerated solution (N_2, 30 minutes) of 140 mL of glacial acetic acid, 14 mL of acetic anhydride, and 2 mL of triethylammine. This solution was allowed to heat while stirring to reflux until the salt dissolved (45 minutes). To this solution 2.917 g of $Mo_2(O_2CCH_3)_4$ was added. The system was, then, heated under reflux while stirring for 7 days. The solution was allowed to cool to room temperature, and 200 mL of distilled water was added. The solution was, then, vacuum filtered using a fine porosity glass frit funnel and then poured on an acidified Dowex 50X2-200 cation

exchange column. The column was, then, rinsed with water which caused a red band to form. The red band was eluted with 1.0 M CF_3SO_3. The eluted band was determined to be Mo_2W by measuring the intensity of absorption band at 450 nm of the cluster. The eluent was placed in the fume hood to slowly evaporate. The air stable red crystals of $[Mo_2WO_2(O_2CCH_3)_6(H_2O)_3](CF_3SO_3)_2$ were obtained. The reaction proceeds stoichiometrically according to:

$$Mo_2(O_2CCH_3)_4 + Na_2WO_4 \rightarrow [Mo_2WO_2(O_2CCH_3)_6(H_2O)_3](CF_3SO_3)_2$$

INSTRUMENTATION

The water content in the ionic liquid was determined using a Denver Instrument Karl Fischer Titrator with a Model 260 titrator controller. 50 microliters of liquid was injected into the titrator using a glass syringe with a stainless steel needle. The syringe was washed in ethanol prior to use and dried in an oven overnight set at approximately 45^{o}C before use.

Cyclic Voltammetry was performed with a platinum working electrode, a Ag | AgCl reference electrode, and a platinum axillary electrods. Measurements were taken using EG&G Princeton Applied Research (PAR) 173 potentiostat/galvonastat equipped with a PAR 175 universal programmer. The analog data was converted to digital data using a MacLab/4 Analog Digital Instruments interface. The data was recorded using Scope V3.1 software and echem V1.5 software after digital conversion. 2 mL of $EMImBF_4$ was placed in a micro cyclic voltammetry cell. An electrochemical cell is shown in Figure 21.

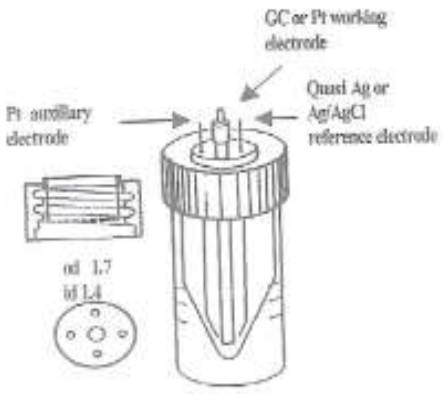

Figure 21. Electrochemical cell with working electrode as platinum, reference electrode as Ag | AgCl, and auxillary electrode as platinum

III. RESULTS AND DISCUSSION

The objective of this work was to synthesize a mixed metal trinuclear cluster, $Mo_2WO_2(O_2CCH_3)_6$, and investigate its electrochemical properties in $EMImBF_4$ ionic liquid. Thus proposing that the $Mo_2WO_2(O_2CCH_3)_6$ cluster could be reduced on a platinum electrode to form a Mo_2W layer, which could change the redox properties of the platinum electrode of an ethanol fuel cell.

SYNTHESIS OF $[Mo_2WO_2(O_2CCH_3)_6(H_2O)_3](CH_3SO_3H)_2$

The mixed metal cluster of $[Mo_2WO_2(O_2CCH_3)_6(H_2O)_3](CH_3SO_3H)_2$ was obtained through a reaction of $Mo_2(O_2CCH_3)_4$ dimer with WO_4^{2-} in acetic acid.

$$Mo_2(O_2CCH_3)_4 + Na_2WO_4 \xrightarrow{CH_3SO_3H} [Mo_2WO_2(O_2CCH_3)_6(H_2O)_3](CH_3SO_3H)_2$$

Figure 22 shows the structure of $[Mo_2WO_2(O_2CCH_3)_6(H_2O)_3](CH_3SO_3H)_2$ cluster.

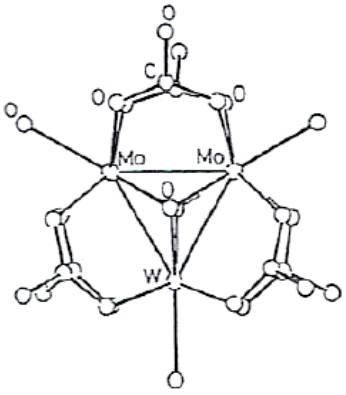

Figure 22. Structure of $Mo_2WO_2(O_2CCH_3)_6(H_2O)_3](CH_3SO_3H)_2$ cluster

The structure contains a triangular unit that is composed of two Mo atoms and one W atom. There are two oxygen atoms above and below the plane. Two $CH_3CO_2^{2-}$ ligands bridge each side of the triangular unit, and three water molecules coordinate its three metal sites. Three metal to metal single bonds are formed when each metal atom contributes two electrons to give an oxidation state of +4.

Metal clusters have been found to be good catalysts because the metal atoms in the cluster resemble the atoms on the surface of a metal. One can adjust their properties by changing the kind of ligands and geometry of the cluster ligand unit.

SYNTHESIS OF $EMImBF_4$

The synthesis of EMImBF4 takes place in a two step process. In the first step, methylimidazole was reacted with chloroethane to obtain EMImCl.

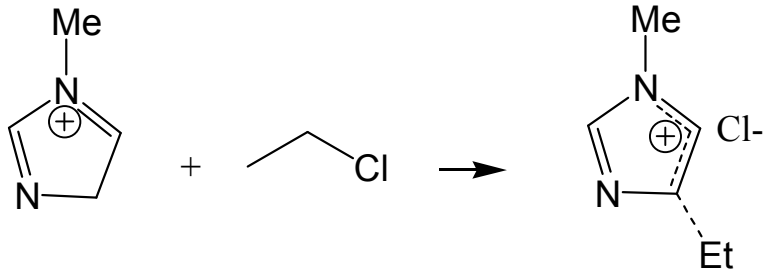

In the second step, the Cl^- anion was replaced with the BF_4^- anion using $NaBF_4$ via:

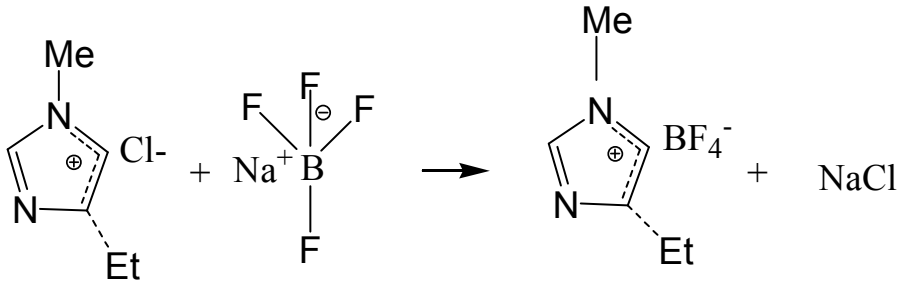

Complete removal of chloride ions was achieved by potentiometric titration with $AgBF_4$. The ionic liquid was evacuated to remove the excess water. After drying, the content of water in the ionic liquid was determined using Karl Fischer coulometric titration.

Figure 23 shows an infrared spectrum of $EMImBF_4$ containing approximately 600 ppm of H_2O. The infrared spectrum was used to confirm the amount of water in the $EMImBF_4$. It was, also, compared to former work to verify that each of the peaks were comparable.

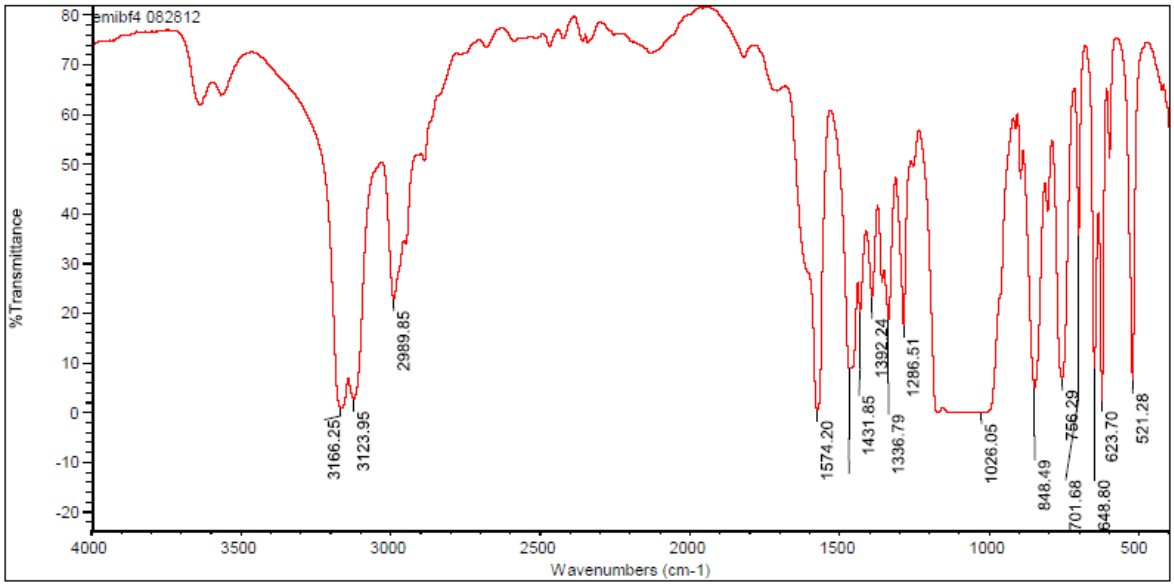

Figure 23. Infrared spectrum of $EMImBF_4$ with 600 ppm of H_2O

ELECTROCHEMISTRY OF $EMImBF_4$

Cyclic voltammetry was used to detect the presence of impurities such as H_2O and chloride ions. Figure 24 shows the cyclic voltammetry of $EMImBF_4$ after drying one day on high vacuum.

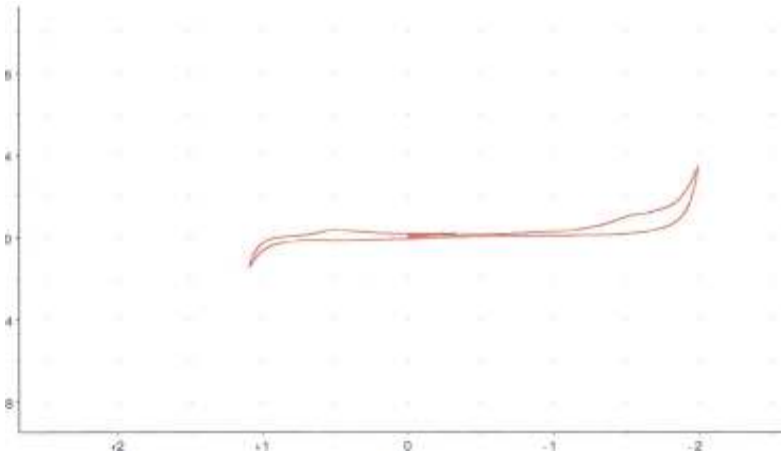

Figure 24. $EMImBF_4$ after only one day on high vacuum

It was clearly seen by the peaks present at +1.5 V and -1.5 V on the cyclic voltammogram that chloride ions and water were still present. The chloride ions were removed by reaction with silver ions and the ionic liquid was dried on high vacuum for two more days. Figure 25 shows the cyclic voltammogram after chloride ion and water removal had taken place.

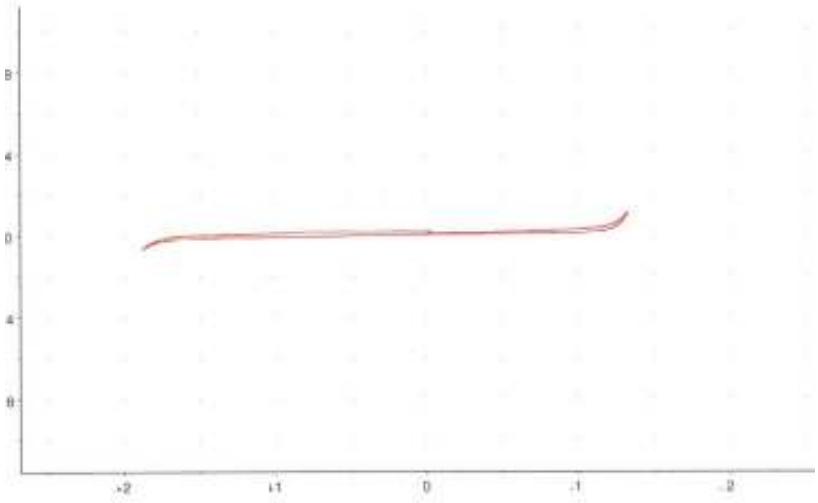

Figure 25. Cyclic voltammogram of $EMImBF_4$ with 600 ppm of H_2O

A potential window of 3.2V was obtained by the pure $EMImBF_4$. The irreversible oxidation peak at -1.5 V that can be seen in Figure 24 cannot be seen in Figure 25, so this confirms the absences of chloride ions.

THE IDENITITY OF $Mo_2WO_2(O_2CCH_3)_6$

The cluster units could be confirmed by their UV and NMR spectral data. Figure 26 and 27 show the electronic spectra of the cluster dissolved in H_2O and $EMImBF_4$. In Figure 26, the noise that appears in the 200-300 nm range is due to cuvette absorbance. Absorbance in this spectral range is not accurate and not considered.

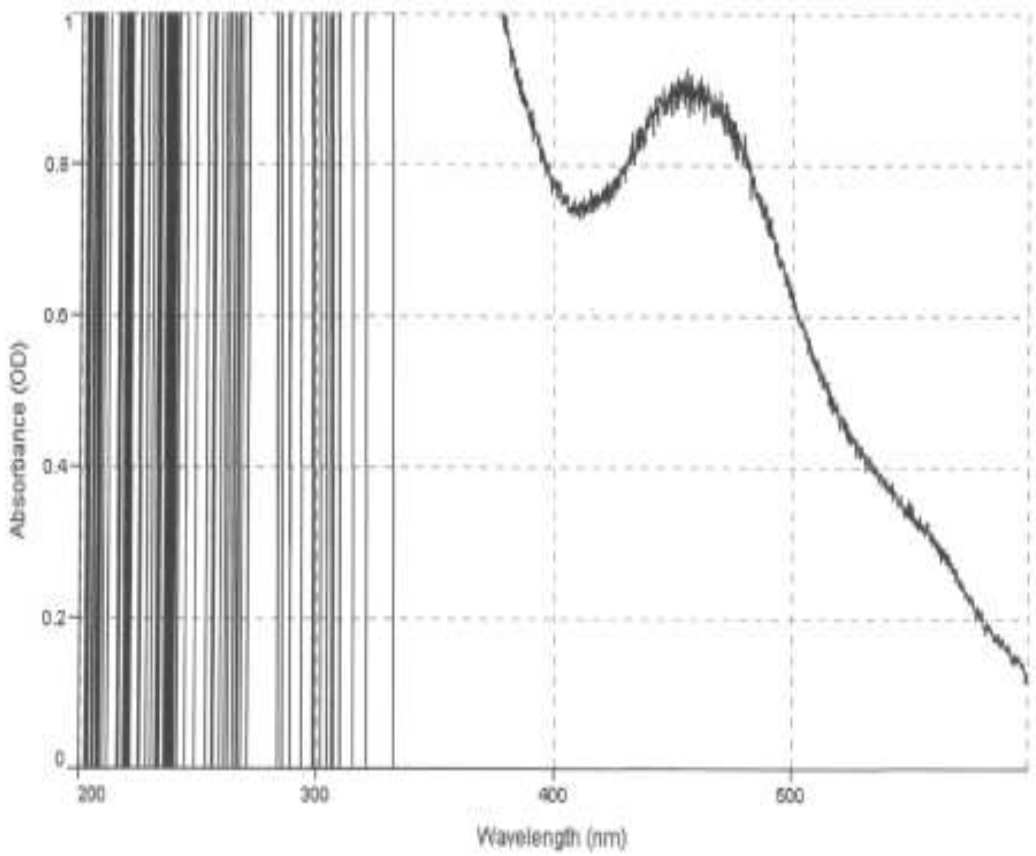

Figure 26. Electronic spectra of $[Mo_2WO_2(O_2CCH_3)_6(H_2O)_3](CH_3SO_3H)_2$ dissolved in H_2O

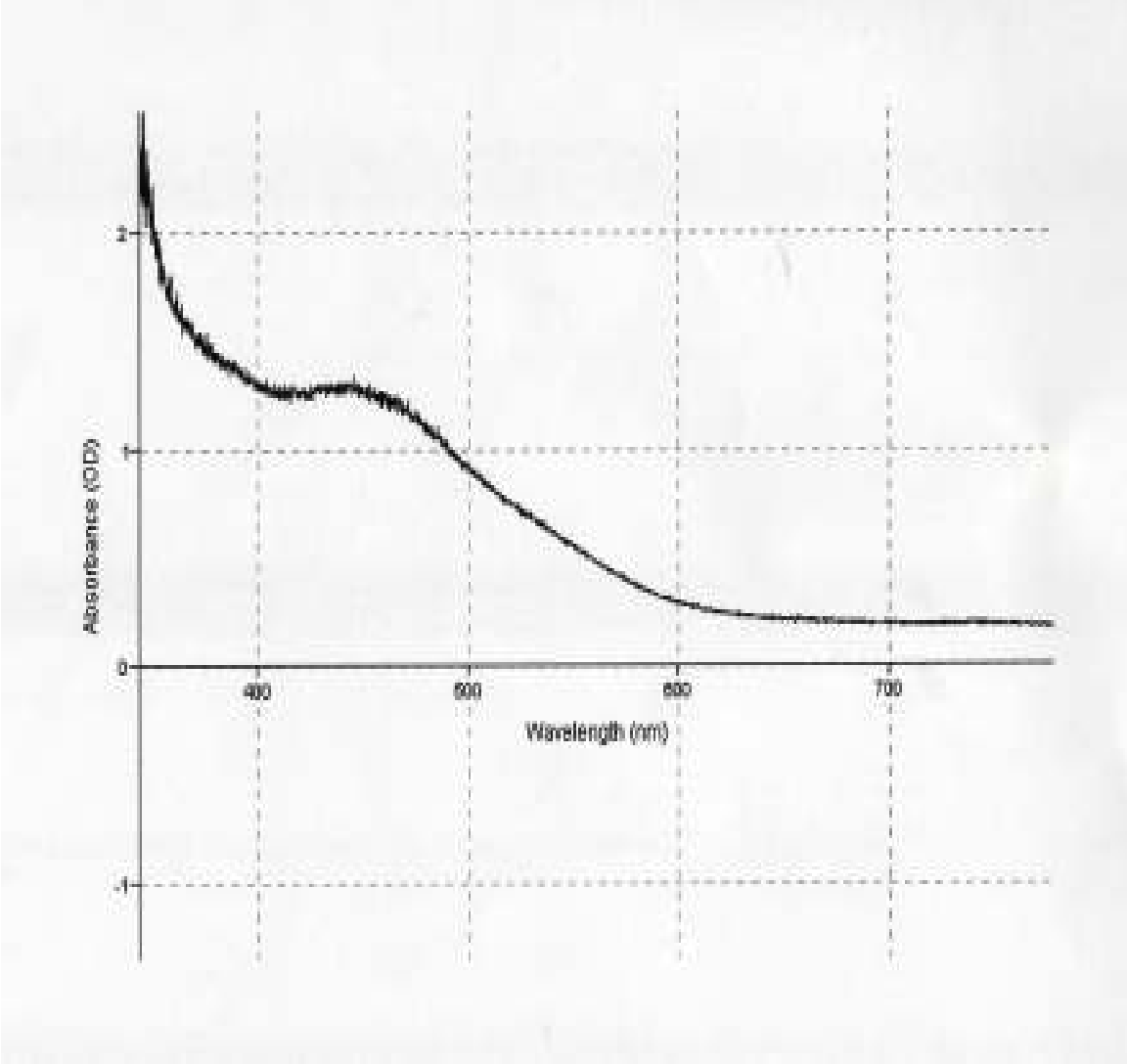

Figure 27. Electronic spectra of $[Mo_2WO_2(O_2CCH_3)_6(H_2O)_3](CH_3SO_3H)_2$ dissolved in $EMImBF_4$

From Figure 26 and 27, it can be seen that the electronic spectra of the trinuclear cluster dissolved in $EMImBF_4$ and H_2O are identical. They both show an absorption band at 450 nm, which suggests that the same cluster species is obtained when dissolved in the ionic liquid or in water.

Figure 28 and Figure 29 show the electronic spectra for $Mo_3O_2(OAc)_6(H_2O)_3(CF_3COO)_2$ and $W_3O_2(OAc)_6(H_2O)_3(CF_3COO)_2$ respectively dissolved in $EMImBF_4$.

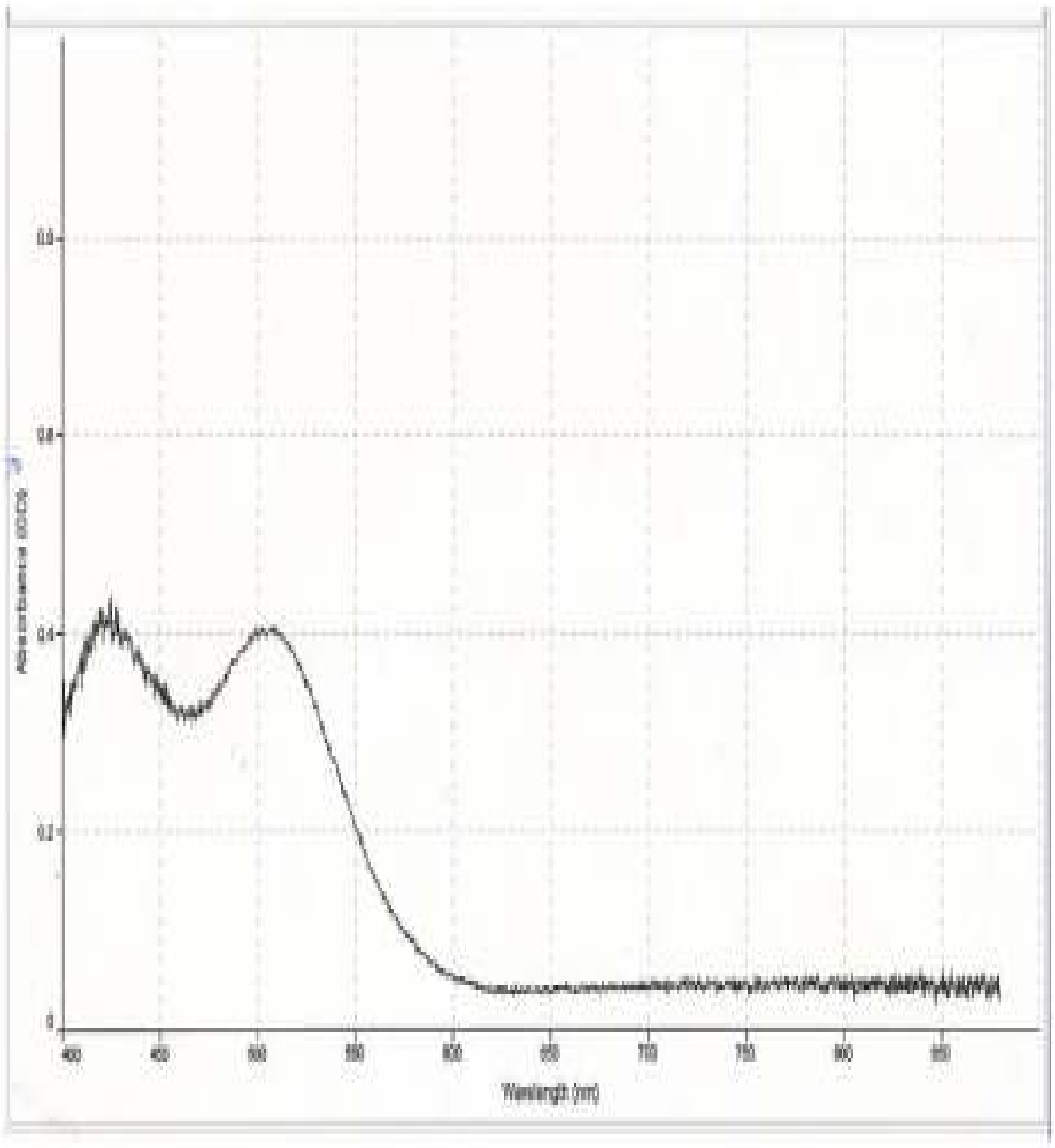

Figure 28. Electronic spectra of $Mo_3O_2(OAc)_6(H_2O)_3(CF_3COO)_2$ in $EMImBF_4$

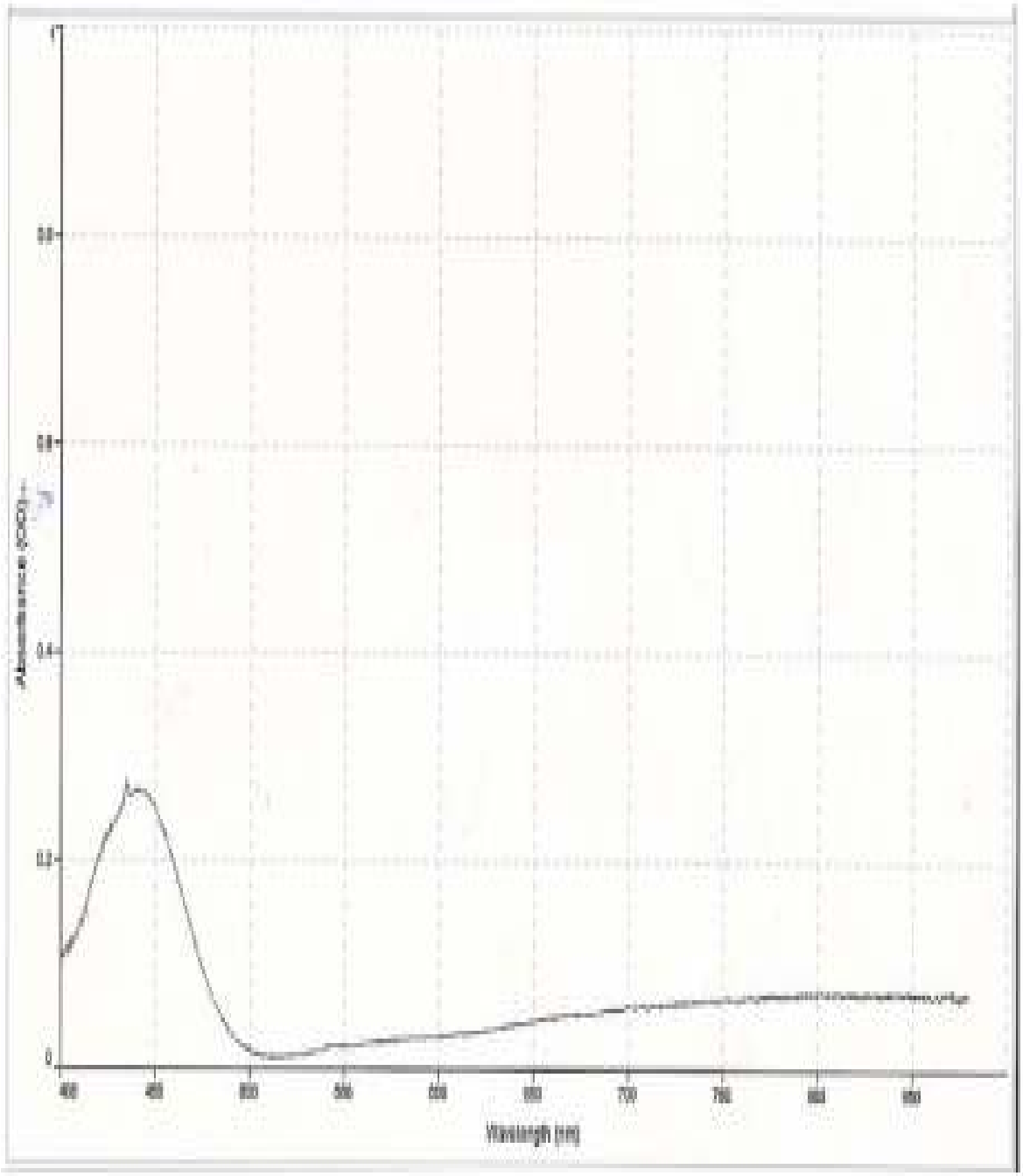

Figure 29. Electronic spectra of $W_3O_2(OAc)_6(H_2O)_3(CF_3COO)_2$ in $EMImBF_4$

All three clusters show absorption bands in the 350-600 nm range. Table 6 shows the comparison of the electronic spectra for each cluster.

Compound	Wavelength (nm)
$[Mo_2WO_2(O_2CCH_3)_6(H_2O)_3](CH_3SO_3H)_2$	450
$Mo_3O_2(OAc)_6(H_2O)_3(CF_3COO)_2$	436 516
$W_3O_2(OAc)_6(H_2O)_3(CF_3COO)_2$	380

Table 6. Comparison of electronic spectra of clusters

Proton NMR was done each of the three metal clusters:

$[Mo_2WO_2(O_2CCH_3)_6(H_2O)_3](CH_3SO_3H)_2$, $Mo_3O_2(OAc)_6(H_2O)_3(CF_3COO)_2$, and $W_3O_2(OAc)_6(H_2O)_3(CF_3COO)_2$. Figure 30-32 shows the spectra for each cluster obtained in D_2O.

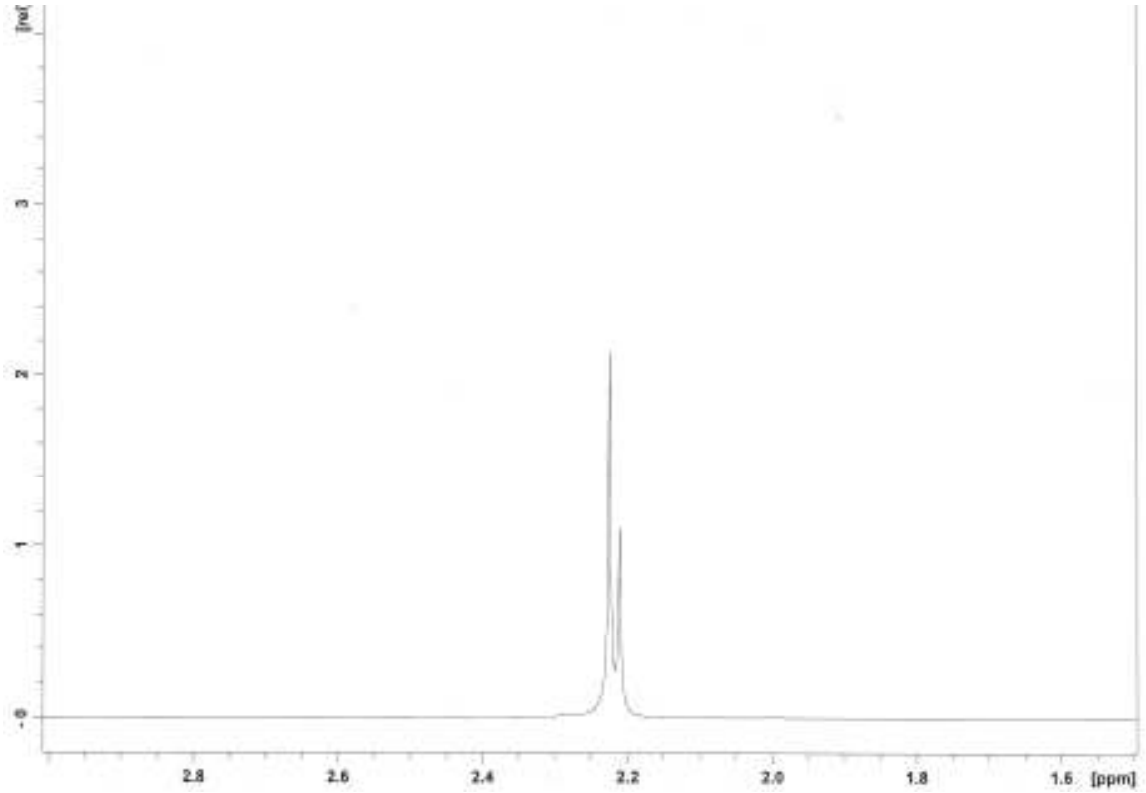

Figure 30. NMR spectra for $[Mo_2WO_2(O_2CCH_3)_6(H_2O)_3](CH_3SO_3H)_2$ in D_2O

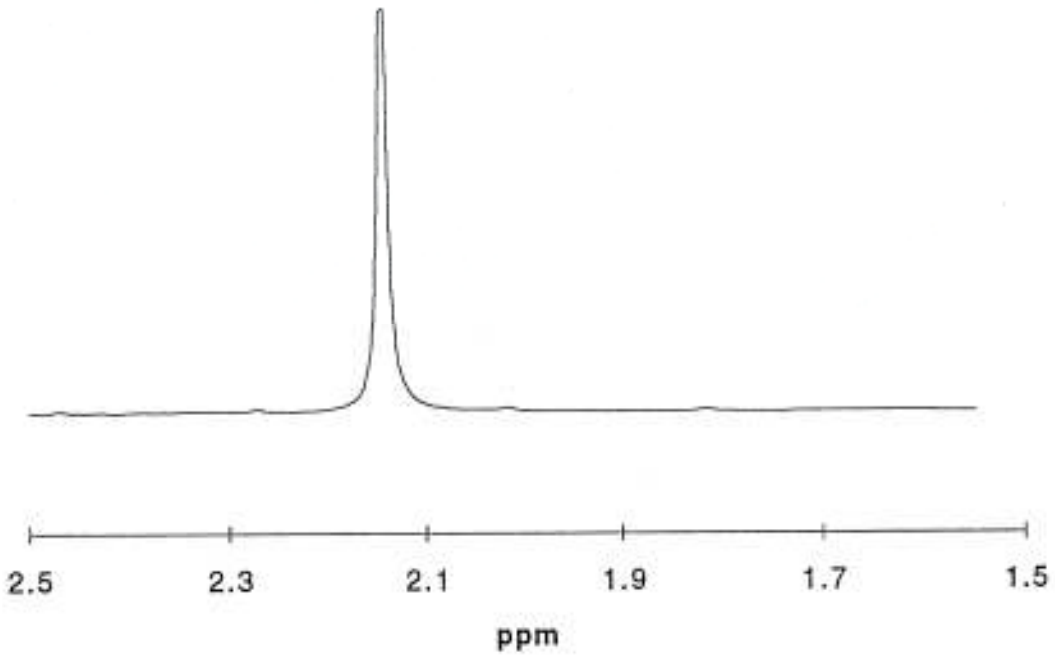

Figure 31. NMR spectra for $Mo_3O_2(OAc)_6(H_2O)_3(CF_3COO)_2$ in D_2O

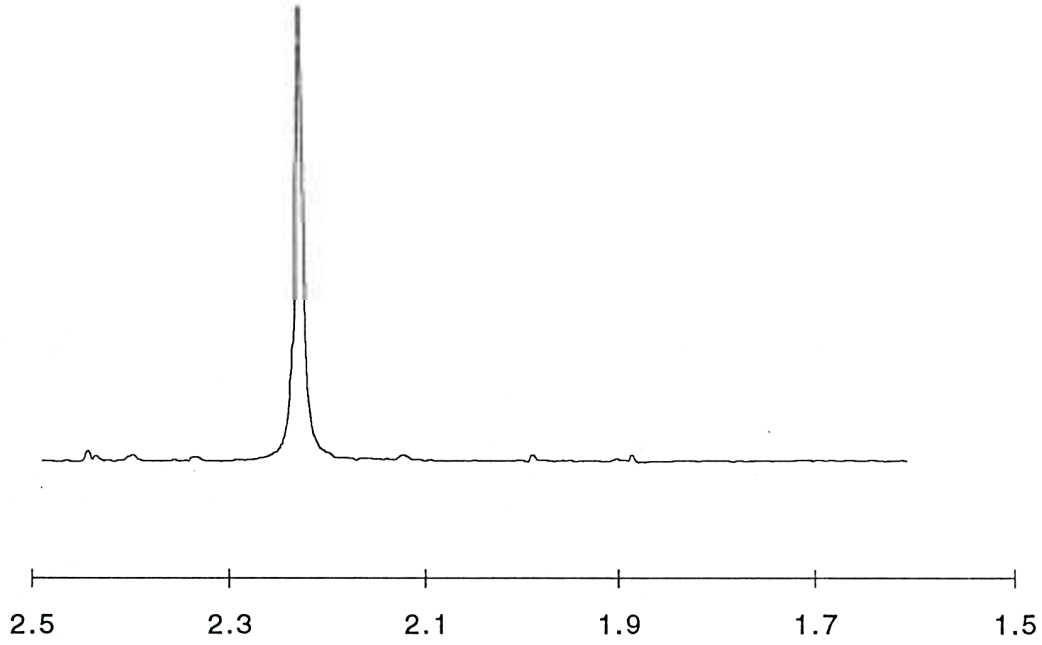

Figure 32. NMR spectra for $W_3O_2(OAc)_6(H_2O)_3(CF_3COO)_2$ in D_2O

$Mo_3O_2(OAc)_6(H_2O)_3(CF_3COO)_2$ and $W_3O_2(OAc)_6(H_2O)_3(CF_3COO)_2$ both show one methyl singlet at 2.14 and 2.23 ppm respectively.

$Mo_2WO_2(O_2CCH_3)_6(H_2O)_3](CH_3SO_3H)_2$ gives two singlets at 2.21 and 2.23 ppm. Table 7 shows the comparison of the NMR spectra for each cluster This NMR spectra along with the electronic spectra is evidence that $[Mo_2WO_2(O_2CCH_3)_6(H_2O)_3](CH_3SO_3H)_2$ is a mixed metal cluster and not a mixture of $Mo_3O_2(OAc)_6(H_2O)_3(CF_3COO)_2$ and $W_3O_2(OAc)_6(H_2O)_3(CF_3COO)_2$ was obtained.

Compound	Ppm
$[Mo_2WO_2(O_2CCH_3)_6(H_2O)_3](CH_3SO_3H)_2$	2.21 2.23
$Mo_3O_2(OAc)_6(H_2O)_3(CF_3COO)_2$	2.14
$W_3O_2(OAc)_6(H_2O)_3(CF_3COO)_2$	2.23

Table 7. Comparison of NMR spectra of trinuclear clusters

ELECTROCHEMISTRY OF $Mo_2WO_2(O_2CCH_3)_6$

Figure 33 shows the cyclic voltammogram of $Mo_2WO_2(O_2CCH_3)_6(H_2O)_3](CH_3SO_3H)_2$ dissolved in $EMImBF_4$.

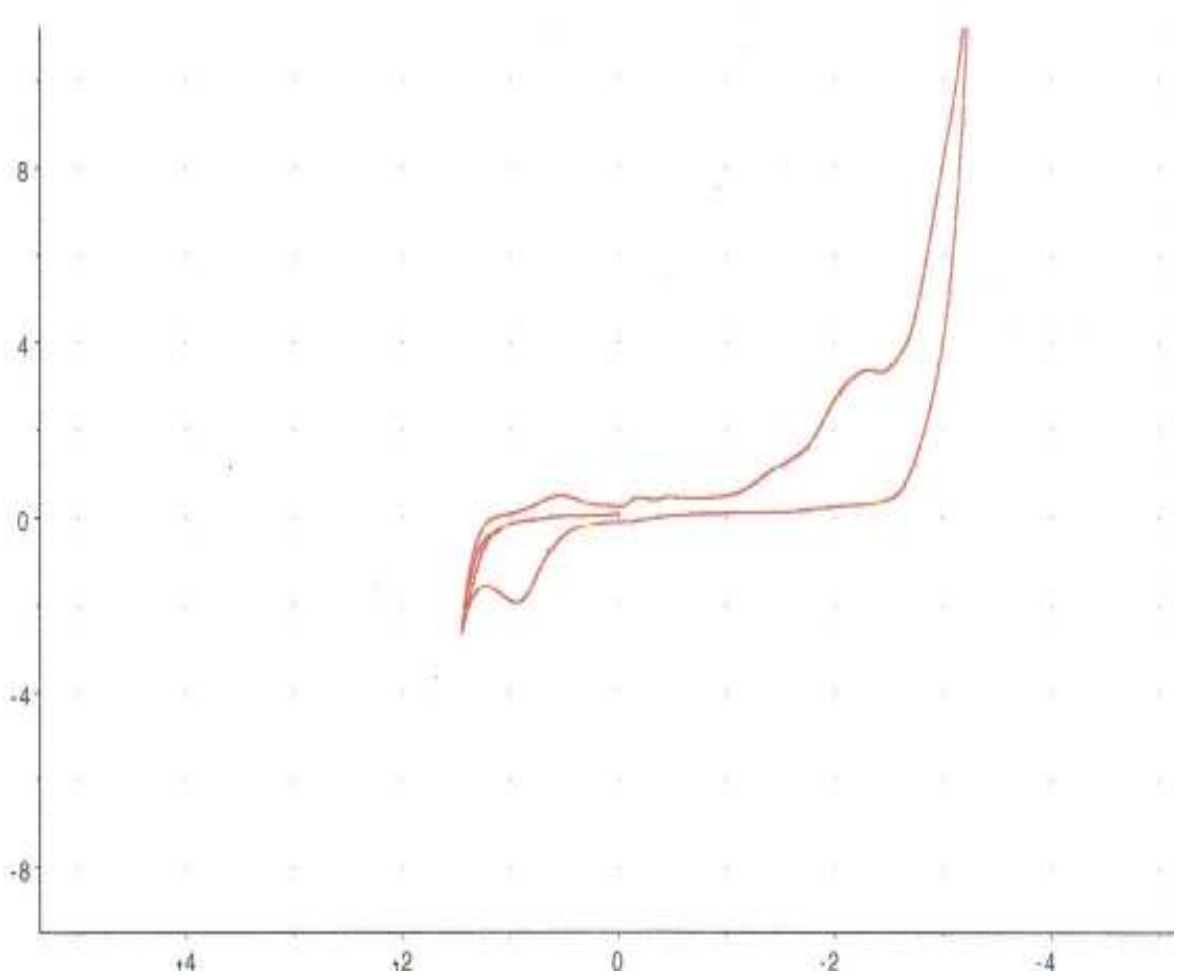

Figure 33. Cyclic voltammogram of $Mo_2WO_2(O_2CCH_3)_6(H_2O)_3](CH_3SO_3H)_2$ dissolved in $EMImBF_4$

On the initial positive potential sweep from 0 to 2.0 V, no oxidation process was observed until the background of $EMImBF_4$ was observed. This indicates that no oxidation of $Mo_2WO_2(O_2CCH_3)_6$ was occurring. On the initial negative sweep, two reduction peaks at -1.30 V and the larger one at -2.2V were observed. Both of these reduction peaks are irreversible because no re-oxidation was observed on the reverse sweep. They probably correspond to multiple reductions of the $Mo_2WO_2(O_2CCH_3)_6$ trimer. On the continuing positive sweep, a new oxidation peak at 1.0 V was observed. This oxidation peak is electrochemically irreversible and probably corresponds to the re-

oxidation of the metal. Controlled potential reduction of $Mo_2WO_2(O_2CCH_3)_6$ at -2.0 V gives an oxidation peak of the oxidation of $Mo_2WO_2(O_2CCH_3)_6$. A picture of the platinum electrode before and after controlled reduction is shown in Figure 36. It is clearly visible that the black reduction product is probably a Mo_2W deposit.

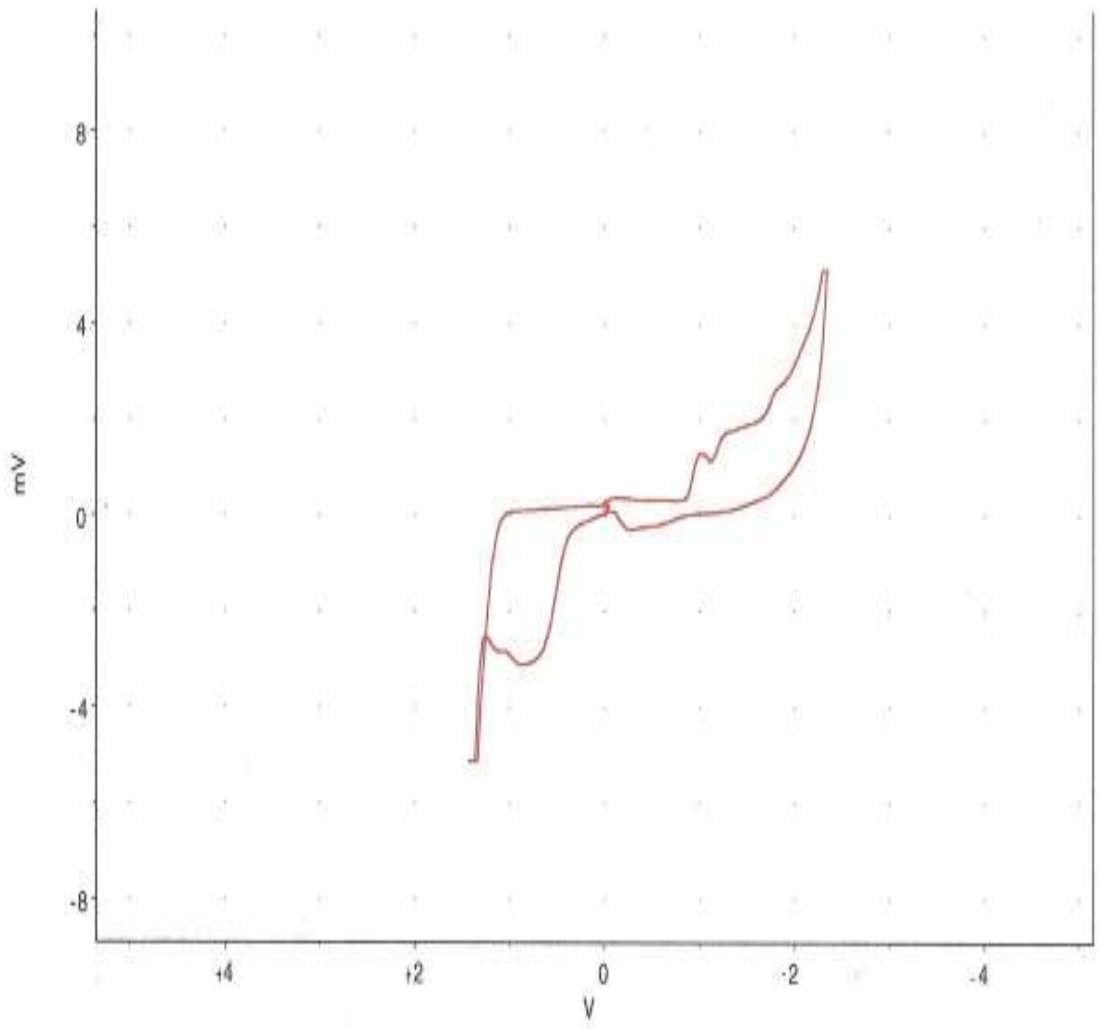

Figure 34. Cyclic voltammogram after 24 hours of reduction

It is clearly seen that the oxidation peak at +0.5 V is larger than the oxidation peak at +1.0 V before constant reduction took place. Reduction peaks are still seen at -1.0 V, -1.3

V, and -1.9 V. This means that reduction has not completely occurred. The cell was put back on constant reduction at -1.25 V for another 24 hours.

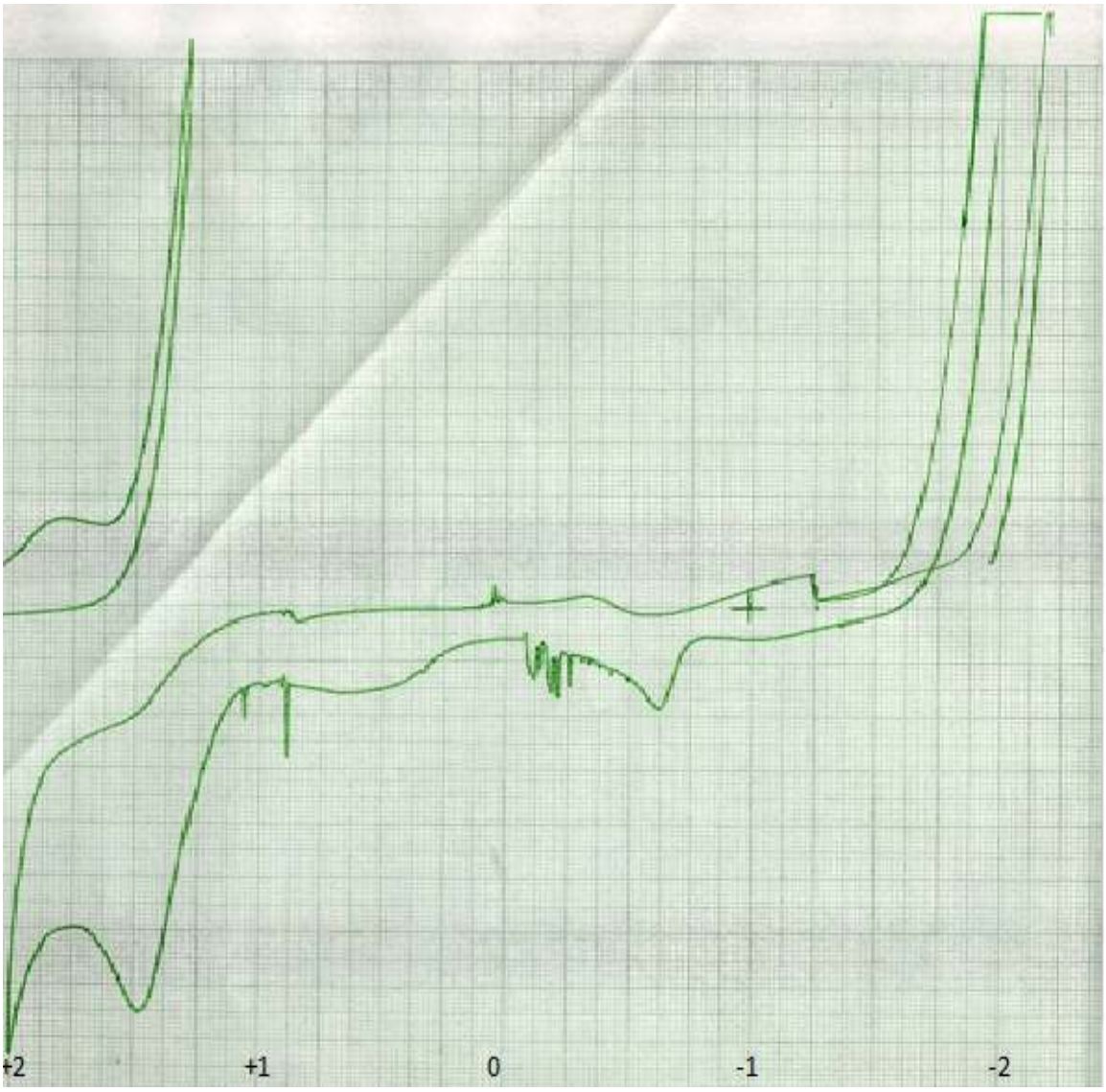

Figure 35. Cyclic voltammogram after reduction

It is seen in Figure 35, that there is a very large oxidation peak with no reduction peaks. This means that reduction has completely occurred.

A. After constant reduction B. Before constant reduction

Figure 36. Platinum electrode before and after controlled reduction

IV. CONCLUSION

The electrochemical properties of a trinuclear mixed metal cluster, $Mo_2WO_2(O_2CCH_3)_6$, was investigated in $EMImBF_4$ ionic liquid. The ionic liquid has a wide potential window, and allows the observation of the redox properties of $Mo_2WO_2(O_2CCH_3)_6$.

$Mo_2WO_2(O_2CCH_3)_6$ was prepared from $Mo_2(O_2CCH_3)_4$ dimer and sodium tungstate. The identity of the cluster was confirmed by the UV and NMR spectral data.

The electrochemistry shows that trinuclear cluster could be reduced to metal by reduction at -2.0 V.

Electrolysis showed the deposit of the $Mo_2WO_2(O_2CCH_3)_6$ cluster onto the platinum electrode.

While the $Mo_2WO_2(O_2CCH_3)_6$ cluster seems to be an option for a platinum free catalyst, future work will need to be done to prove its efficiency in the ethanol fuel cell.

V. REFERENCES

1. Harris, T. *Electrochemistry of Trinuclear Metal Clusters of Molybdenum and Tungsten in 1-Ethyl-3-Methylimidazolium Tetrafluoroborate*. 2008.

2. Wanamaker, M. *Syntheses and Electrochemistry of Trinuclear Metal Clusters of Tungsten and Molybdenum*. 1998.

3. Allain, E. *J Chem Technol Biotechnol*. 2007, 82, 117-120.

4. Tayal, J, Rawat, B, Basu, S. *International Journal of Hydrogen Energy*. 2011, 36, 14884-14897.

5. Pramanik, H., Basu, S. H. *Chemical Engineering and Processing.* 2010, 49, 635-642.

6. Li, Y.S., Zhao, T.S. *International Journal of Hydrogen Energy*. 2012, 37, 4413-4421.

7. Tayal, J., Rawat, B., Basu, S. *International Journal of Hydrogen Energy*. 2012, 37, 4597-4605.

8. Lamy, C., Lima, A., LeRhun, V. Delime, F., Coutanceau, C., Leger, J. *Journal of Power Sources*. 2002, 105, 283-296.

9. Aguirre, C., Cisternas, L., Valderrama, J. *Int J Thermophys*. 2012, 33, 34–46.

10. Cartert, E., Goddard, W. *J. Phys. Chem.* 1988, *92,* 2109-2115.

11. Kulikovshy, A.A. *Electrochimica Acta*. 2012, 79, 52– 56.

12. Rosenthal, N., Vilekar, S., Datta, R. *Journal of Power Sources*. 2012, 206, 129–143.

13. Ferreira, A.F., Simoes, A., Ferreira, A. Andre F. *J. Chem. Thermodynamics*. 2012, 45, 16–27.

14. Kochel, A. *Inorganic Chemistry Communications*. 2007, 10, 1440–1443.

15. Shoaf, J. *Thermal and Electrochemical Characterization of Cathode Materials for High Temperature Lithium-Ion Batteries in Ionic Liquids.* 2010.

REFERENCES (CONTINUED)

16. Thimmappa, B.H.S. *Journal of Cluster Science*, Vol. 7, No. 1, 1996.

17. Adams, R., Boswell, E., Miao, S., Sanval, S. *Journal of Cluster Science*, Vol. 16, No. 2, 2005.

18. U.S. Energy Information Administration. Annual Energy Review 2010. October 2011

19. Jung, B., Meyer, G., Herdtweck, E. *ibid.*1991, 604, 27- 33.

20. Dyar, H. *The Synthesis, Electrochemical, and Thermal Characterization of 1-Ethyl-3Methylimidazolium and 1-Ethyl-2-Metylpyrazolium Based Room Temperature Ionic Liquids. 2001*.